"Non-invasive" portable laser ablation sampling for lead isotope analysis of archaeological silver

Merkel, S. W.; D'Imporzano, P.; Van Zuilen, K.; Kershaw, J.; Davies, G. R.

Link to publication in VU Research Portal

Check for updates

"Non-invasive" portable laser ablation sampling for lead isotope analysis of archaeological silver: a comparison with bulk and *in situ* laser ablation techniques†

S. W. Merkel, [ID] *ab P. D'Imporzano,c K. van Zuilen, [ID] c J. Kershaw [ID] b and G. R. Davies [ID] c

The main factor restricting lead isotope analysis of metals from museum collections is the requirement for physical material. Hence, there are major incentives for developing minimally invasive methods for lead isotope analysis that are accurate and precise enough to reveal historical information about artefacts and their origin. Portable laser ablation (pLA), collecting microscopic samples on Teflon filters, has four key benefits. It produces no visual impact to the artefacts, does not require transport of artefacts to laboratory facilities, there are no artefact size restrictions, and samples are processed under clean laboratory conditions allowing Pb purification prior to measurement by solution MC-ICPMS. To validate the efficacy of the pLA technique on silver, nine matrixed-matched commercial, in-house and archaeological reference materials were sampled and analysed multiple times (9–10). The pLA mean analyses (±2SD) were all consistent with inter-laboratory bulk analyses. The digestion of sample filters produces precisions that are consistently more than five-times better than *in situ* nsLA-MC-ICPMS and are the same order of magnitude expected for bulk samples processed in different laboratories.

Introduction

The importance of understanding the exchange and trade of archaeological materials, coupled with the growing availability of inductively coupled plasma mass spectrometry (ICPMS) is leading to an increasing application of trace element and/or isotopic analysis in archaeology. For artefacts made of an array of non-ferrous metals, the lead isotope system is valuable because of its enormous potential in tracking the flow of metals over time and space.[1–3] A factor that greatly limits the scale and scope of lead isotope studies of ancient metals is the access to sample material. Sample availability is particularly acute for silver and other rare archaeological metals, which, because of their high cultural value and paucity, are frequently barred from invasive sampling techniques. There has been a major creative drive to develop minimally and non-invasive methods to push analytical capabilities within the field of archaeology for more than half a century (examples for precious and copper alloys[4–13]). The methodological advancement of mass

spectrometry techniques in archaeology is not only concerned with the ability to measure smaller samples with improved accuracy and precision but also curatorial factors such as the impact to the artefact and where physical sampling takes place.[13,14] Laser ablation (LA) is the least invasive technique developed for metal artefacts that is capable of collecting a physical sample. Laser ablation pits ≤ 100 μm in diameter are indistinguishable from natural surface imperfections to the naked eye, and, in terms of non-invasiveness, are a substantial improvement on acid leaching and oxidation techniques, which irreversibly alter the surface of the metal, and micro drilling and abrasion with quartz, which leave visible traces, unless carefully restored by a conservator.

A laser system can be directly coupled to an ICP mass-spectrometer for online *in situ* analysis but there are several drawbacks to this approach. It requires the transport of artefacts from museums to suitable laboratory facilities, demanding careful planning and exposing the artefacts to added risks. The artefacts need to be placed in sample chambers of restricted size (generally <10 × 10 × 1.5 cm), limiting the size and types of objects that can be analysed. Matrix-matched reference materials are required for method development and especially instrument calibration and mass bias correction, which requires analysis of artefacts prior to LA sampling. *In situ* LA-Multi-collector (MC)-ICPMS systems used for lead isotope analysis are almost exclusively equipped with

a Deutsches Bergbau-Museum Bochum, Research Division, Herner Str. 45, Bochum 44787, Germany. E-mail: swmerkel@hotmail.com

b University of Oxford, School of Archaeology, 2 South Parks Road, Oxford OX1 3TG, UK

c Faculty of Science, Vrije Universiteit, 1085 De Boelelaan, Amsterdam 1081 HV, The Netherlands

† Electronic supplementary information (ESI) available. See DOI: 10.1039/d1ja00342a

nanosecond lasers.[5,13,15–17] These lower frequency lasers produce a relatively heterogeneous particle size distribution and can cause a degree of inter-elemental and isotopic fractionation.[18–20] Combined with the low abundance of ^{204}Pb and isobaric interferences, this makes it difficult to measure ratios relative to ^{204}Pb, which leads to long-term precision of 0.3–0.4% (2 relative standard deviations).[5,13,16,17] Precision in this range is sufficient to answer a range of archaeological questions but is not ideal for provenance studies, for which, conventionally, precision and accuracy better than 0.1% 2RSD are desired.[3]

An indirect filter sampling system using a portable LA (pLA), as successfully applied on various mediums for the measurement of lead isotope ratios (pigments, metallic lead, galena[14]), other isotope systems (stone[21]) and elemental concentrations (copper,[6] pigments, gold, glass[22]), has the potential to circumvent many of the problems associated with *in situ* lead isotope analysis of silver by laser ablation. With pLA, the laser can be brought to the artefacts, permitting sampling of invaluable and vulnerable objects inside a museum supervised by a curator, thus alleviating the need for transport to laboratory facilities. The system also provides an opportunity to acquire lead isotope data from collections in locations with no available isotopic facilities. Ablated sample material collected on filters is processed under clean laboratory conditions, purified to separate Pb from the matrix and measured in solution form. Thus, analytical interference related to the sample matrix and melting behaviour, which impair *in situ* nsLA analyses, are avoided. To test the practicality, accuracy and precision of the indirect pLA method for the capture and measurement of lead isotope ratios in silver, nine matrixed-matched commercial, in-house and archaeological reference materials were sampled by pLA in 9–10 repetitions and analysed together with bulk samples at the Vrije Universiteit (VU), Amsterdam. These data are compared with the results of the same reference materials from external laboratories using *in situ* LA MC-ICPMS and bulk MC-ICPMS.

Methods

Reference materials

This study uses a set of nine silver reference materials. One is commercially available (MBH 133X-AGA3, batch A). Six were produced in house: three by melting silver together with metallic lead and three by extracting silver from ore minerals through smelting and cupellation. The final two are samples of archaeological silver used as inter-laboratory reference materials (Table 1). The methods of manufacture of the reference materials produced in house closely follow those outlined in ref. 13 and 23 some being the same materials (RMAgD-1 and RMAgS-1) and others re-homogenised by re-melting (RMAgP-2) or re-made (RMAg981-3) using the same procedure. RMAgN-2 was made from ore but was alloyed with lead to increase the lead content. RMAg981-3 contains 0.9 wt% of the lead isotope standard NIST Pb 981 alloyed as a metal with high purity silver (MBH 131X AGP4, Pb = 5 ppm). The microstructures of the commercial and in-house manufactured reference materials are shown in Fig. 1. The silver that underwent cupellation (for example RMAgD-1 and RMAgS-1) was more homogeneous and had smaller (sub-micron) lead-rich phases than silver that was alloyed with metallic lead. The most heterogeneous reference material in terms of lead content is RMAgN-2. The silver contents of the reference materials range from 91 to 99 wt%. Copper is found in trace amounts (<1000 ppm) up to *ca.* 5.5 wt%. and lead from 0.36 to 3.5 wt% (Table 1). Minor-to-trace amounts of gold and bismuth are also in the materials. This range of compositions is analogous to many high-purity archaeological silver alloys.

Table 1 List of in-house and commercial silver reference materials. The compositions of the majority were characterised by solution based ICP-QMS using the methods of ref. 23. The two archaeological samples have been characterised in multiple laboratories by ICP-(Q)MS.[28,29] *Lead contents were measured by portable X-ray fluorescence (Niton XL3T Analyzer, Thermo Scientific) on flat clean metal surfaces

|	Reference material	Description/production	Pb (%)	Cu (%)	Au (ppm)	Bi (ppm)	Measurement	Names after Standish *et al.* 2021
1	RMAg981-3	Ag, commercial MBH 131X AGP4 melted with metal NIST981 and cast into water	0.9	<0.1	9	8	Ox-ICPQMS	New version of RMAg981
2	133X-AGA3	Ag, commercial MBH reference material with 5% Cu and minor and trace elements	1.9	4.9	2600	480	MBH-ICPOES	Same
3	RMAgD-1	Ag, produced from smelting galena to lead and cupelling silver ore	0.36	0.1	3	25	Ox-ICPQMS	Ag-Du
4	RMAgN-2	Ag, produced from smelting and cupelling argentiferous galena/remelted with Pb	3.5	<0.1	640	0.2	Ox-ICPQMS	—
5	RMAgS-1	Ag, produced from smelting and cupelling argentiferous galena	2.5	<0.1	5	0.2	Ox-ICPQMS	Ag-Sl
6	RMAgC-1/2	Ag, silver melted with lead and cast into water = 1; remelted and recast = 2	0.4*	<0.1	9	0.5	Ox-ICPQMS	—
7	RMAgP-1/2	Ag, silver melted with lead and cast into water = 1; remelted and recast = 2	0.5*	<0.1	9	120	Ox-ICPQMS	RMAgP-1 = Ag-4817-14
8	RMAg3834	Ag, archaeological sample	0.5	3.4	3900	15	Ave. multi-lab	RM3834
9	RMAg12467	Ag, archaeological sample	1.1	5.5	1900	650	Ave. multi-lab	RM12467
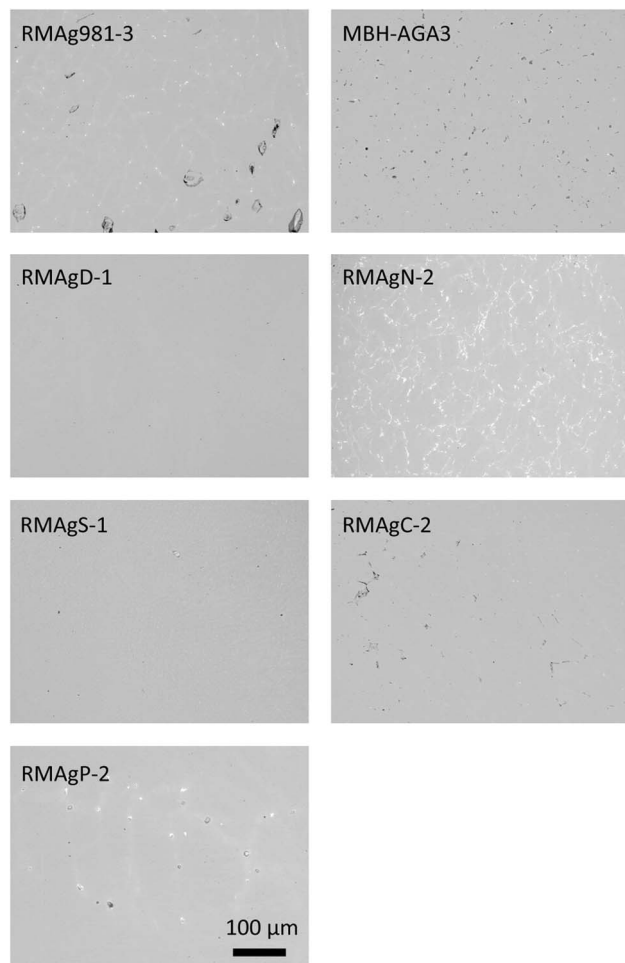
Fig. 1 Scanning electron microscope (SEM) backscatter images showing microstructure of commercial and in-house silver reference materials at ×200 magnification. Lead-rich phases are white, due to their greater density.

Portable laser ablation sampling

The main features of the portable laser ablation sampling system are described in ref. 21 and 22. Sampling took place at the Department of Earth Sciences, VU Amsterdam. The pLA system is composed of a pulsed diode pumped solid-state laser (Wedge HB532, Bright Solutions SRL, Cura Carpignano, Italy), optical laser ablation module, sample holder and membrane pump. The laser produces a wavelength of 532 nm with a pulse duration of <1 ns. The pulse frequency can be adjusted between 1–10 000 Hz and 100 Hz was used for sampling. The laser beam output has a diameter of 1 mm and output energy of 1.3 mJ. The beam is focused by an aspheric lens mounted on a x/y translation stage. This study used a 2 m optical fibre (QP450-2-XSR, Ocean Optics Inc., Dunedin, FL, USA) with a core diameter of 450 μm. The laser produces a homogenised energy distribution that is focused on the sample surface by two lenses in the ablation module. The beam diameter was ~100 μm diameter with a maximum energy at the sample surface of >1 mJ. The ablated sample is collected on a Teflon filter by suction generated by a miniature oil-free membrane pump. During ablation,

the sample surface is illuminated with a LED ring and observed with a monochromatic CCD camera. The eight-fold magnification allows observation of a 1 mm^2 sample area, so that the exact sampling position and the focal point of the laser can be optimised. Sampling is generally undertaken in a collapsible Perspex box (1.5 × 1.5 × 1.5 m) that is fed by filtered air to reduce environmental dust contamination.

An individual ablation sample is taken in a ninety-second routine, *i.e.*, ~9000 pulses. Samples were collected on hydrophobic PTFE Mitex® membrane filters (LSWP01300, Merck Millipore Corporation, MA, USA) that have a pore size of 5 μm and a porosity of 60%. Filters are 13 mm in diameter with

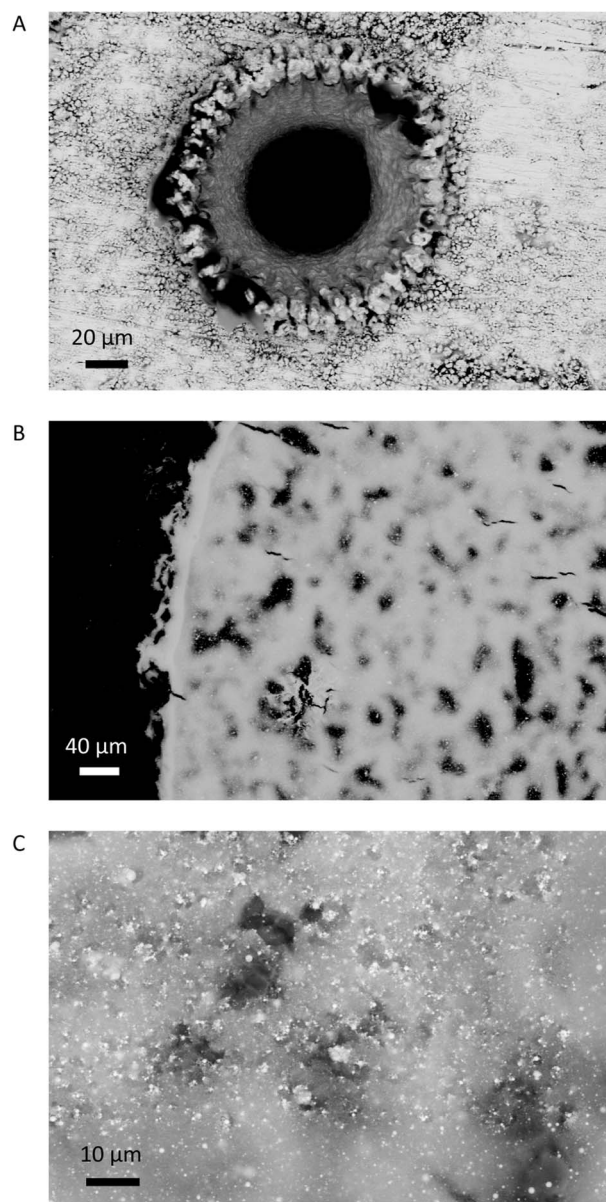**Fig. 2** SEM backscatter images of ablation crater after pLA (RMAg981-3) and ablated material on filter (MBH-133X-AGA3). (A) ×420; (B) ×200; (C) ×1000 magnification. The ablated sample typically consists of sub-micron particles but spherical metallic droplets can be seen with diameters up to ~ 2 μm.

150 | *J. Anal. At. Spectrom.*, 2022, **37**, 148–156

This journal is © The Royal Society of Chemistry 2022

a thickness of 170 μm. All filters were extensively pre-cleaned by placing them in a 15 mL Teflon beaker containing 10 mL of a mixture of 3 M HCl and 0.2 M HF. All Teflonware used in the project was thoroughly pre-cleaned in a procedure, (see ref. 24 and 25 for details). Filters to be used for Pb isotope analysis were further cleaned for >1 week in 10 mL of 1 M HBr at 120 °C. Purified filters are stored and transported in Milli-Q® in acid-cleaned PTFE vials. During sampling, six filters are located in a sample wheel. Before switching to a new filter position, the ablation chamber is cleaned using ethanol and compressed air and the tubing replaced by acid-cleaned tubing, previously cleansed by soaking for 2 days in 10% HNO_3 and 2 days in 1 M HBr.

Five combined environment and filter blanks were prepared between sampling the silver by pumping air through the filter for 20 min. Examples of ablation and sample accumulation on the filter are shown in Fig. 2. The samples were taken over a period of three days by two different operators. The number of ablations needed per filter were calculated to collect ≥1 μg Pb using an estimated ablation mass of 25 μg and the Pb content of the metal. Pb contents in the range of 0.4 wt% required 10 ablations per filter, while for the highest Pb contents, > 1.5 wt%, material from two ablations were collected per filter (Tables 1 and 2). After sample collection, filters were extracted from the holder on site and stored in acid-cleaned 2 mL centrifuge tubes. The samples were processed in the low blank isotope geochemistry laboratories of the VU Amsterdam.

Sample dissolution

The filters holding the ablated silver were submerged in 1.5 mL 7 M HNO_3 in a class 1000 clean laboratory for sample digestion. The samples were sonicated for 30 minutes in order to achieve full dissolution of the silver. Once the samples were dissolved, the filters were removed using plastic tweezers cleaned with HNO_3 and Milli-Q water between samples. The solutions were decanted into pre-cleaned 7 mL Savillex vials. The extraction of the Pb fraction during the chromatography involves the use of 6–7 M HCl, and if a significant quantity of silver is present, the chromatographic columns can clog as AgCl deposits on the

resin. Therefore, the solutions were treated with 1.5 mL 6–7 M double-distilled HCl and centrifuged for 10 minutes. The samples supernatant solution was separated from the precipitated AgCl and dried down. The samples were then dissolved in 1 mL 7 M double-distilled HBr, placed in centrifuge tubes and centrifuged for 10 minutes. The contents, minus precipitation, were returned to the beaker and dried.

Bulk metal samples (10–20 mg) were weighed and dissolved in 1.5 mL 7 M double-distilled HNO_3 in 7 mL Savillex Teflon beakers. Once fully dissolved, 1.5 mL 6–7 M doubled-distilled HCl was added and dried. Contents were re-dissolved in 1 mL 7 M double distilled HBr and subsequently diluted to 7 mL with MQ, placed in clean 15 mL centrifuge tubes and centrifuged for 4 minutes to force the precipitate to settle. An aliquot was taken equal to 1 μg Pb from each solution and placed in a Savillex beaker. The aliquots were dried down.

The lead fraction of the samples was purified for analysis following the procedure described in ref. 26. In brief, the samples were re-dissolved in 0.3 mL 0.7 M HBr. The solution was then processed by ion-exchange chromatography using AG®1-X8 anion exchange resin (analytical grade, 200–400 mesh, chloride form). Sample repetitions were spread across multiple batches of column separation. The concentration of the Pb fraction was determined by ICPMS. Once Pb concentrations were known, 2 mL 1% HNO_3 solutions were made containing 100 ng of Pb (50 ppb).

The solutions were analysed using a Thermo Scientific Neptune MC-ICPMS using standard sample bracketing (SSB) to correct for instrumental mass fractionation. Data quality was monitored for each batch of analyses with an NBS981 lead solution and two in house internal standard solutions. Blank samples were prepared in exactly the same manner. The analyses of the blank solutions was performed by isotope dilution with a [208]Pb spike solution of known concentration and isotopic composition.

Lead isotope analysis

Lead isotope analyses at the VU Amsterdam facility were performed using a desolvating nebulizer system, CETAC Aridus II,

Table 2 Methods and laboratories used to analyses reference materials. The number of ablations per filter were calculated based on the lead content and the ablation volume in order to collect ≥1 μg Pb

Reference material	Ablations per filter	VU-Amst. pLA filters MC-ICPMS	VU-Amst. bulk MC-ICPMS	U. of Ox. bulk MC-ICPMS	U. of Southampton *in situ* nsLA-MC-ICPMS	Vegacent. Stockholm *in situ* nsLA-MC-ICPMS	U. of Edinburgh *in situ* nsLA-MC-ICPMS	GU-Frankfurt/ Main bulk MC-ICPMS	LU-Hannover *in situ* fsLA-MC-ICPMS
1 RMAg981-3	4	X	X	X	X	X	X	—	—
2 MBH 133X-AGA3	2	X	X	X	X	—	X	—	—
3 RMAgD-1	10	X	X	X	X	X	X	—	—
4 RMAgN-2	2	X	X	X	—	X	X	—	—
5 RMAgS-1	2	X	X	X	X	—	X	—	—
6 RMAgC-1/2	10	X	X	X	X	—	—	—	—
7 RMAgP-1/2	6	X	X	X	X	—	—	—	—
8 RMAg3834	8	X	—	X	—	X	—	X	X
9 RMAg12467	4	X	—	X	X	X	X	X	X

Table 3 Bulk Pb isotope analysis of silver reference materials by MC-ICPMS at the VU Amsterdam

		$^{206}Pb/^{204}Pb$	2SE	$^{207}Pb/^{204}Pb$	2SE	$^{208}Pb/^{204}Pb$	2SE	$^{207}Pb/^{206}Pb$	2SE	$^{208}Pb/^{206}Pb$	2SE
1	RMAg981-3	16.944	0.001	15.501	0.001	36.732	0.002	0.91482	0.00001	2.16774	0.00003
2	MBH 133X-AGA3	17.414	0.001	15.554	0.001	37.299	0.003	0.89320	0.00001	2.14191	0.00003
3	RMAgD-1	18.695	0.001	15.665	0.001	38.811	0.003	0.83792	0.00001	2.07601	0.00003
4	RMAgN-2	18.506	0.001	15.635	0.001	38.629	0.002	0.84490	0.00001	2.08737	0.00003
5	RMAgS-1	18.044	0.001	15.576	0.001	38.078	0.003	0.86325	0.00001	2.11028	0.00003
6	RMAgC-2	18.534	0.001	15.644	0.001	38.494	0.003	0.84404	0.00001	2.07687	0.00003
7	RMAgP-2	20.067	0.002	15.811	0.001	40.943	0.003	0.78790	0.00001	2.04027	0.00003

operating at approximately 4–5 L min^{-1} of Ar sweep gas, 0.01–0.02 L min^{-1} nitrogen and with temperature settings of 110 °C for the spray chamber and 160 °C for the membrane. Lead ion beams were about 0.2 V ppm^{-1} on Faraday cups equipped with 10^{11} Ω amplifiers. A gain calibration was performed once per week. An analysis consisted of one block of 100 cycles of 4 seconds integration time. The Neptune operated with a RF power of 1290 W. Faraday cup detectors were assigned to the following masses: ^{201}Hg L4, ^{202}Hg L3, ^{204}Pb L2, ^{205}Tl L1, ^{206}Pb C, ^{207}Pb H1, ^{208}Pb H2, ^{209}Bi H3. The standard sample bracketing method used a 50 ppb solution of NIST981 before and after each sample. The sample analyses were correct against the values of NIST981 presented in ref. 27. The long-term precision, expressed as 2 times the standard deviations (2SD) over two years, is 0.003 for $^{206}Pb/^{204}Pb$ and $^{207}Pb/^{204}Pb$, 0.011 for $^{208}Pb/^{204}Pb$, 0.0001 for $^{207}Pb/^{206}Pb$ and 0.0003 $^{208}Pb/^{206}Pb$. The lead isotope results are presented in Tables 3, 4 and S1.†

Comparative analyses

The reference materials have been analysed in multiple laboratories using different MC-ICPMS techniques and methodologies (Table 2). Analyses of the same reference materials were carried out by MC-ICPMS at the University of Oxford, Department of Earth Science and by *in situ* nano-second laser ablation MC-ICPMS at the University of Southampton using the methods of ref. 13. A set of analyses of RMAg3834 and RM12467 by solution MC-ICPMS at the Goethe University Frankfurt am Main and femto-second LA-MC-ICPMS at the Leibniz University Hannover is published in ref. 28 and 29. Two studies using nsLA MC-ICPMS were conducted at the Grant Institute, University of Edinburgh and the Vegacenter, Natural History

Museum Stockholm.[16,17] These analyses are presented in Tables S2–S8.† The methodologies used in the three laboratories performing *in situ* nsLA MC-ICPMS datasets were standardized to use a consistent laser beam size rather than adapting the beam size to match signal intensities of bracketing reference materials. Adapting beam size to match signal intensity is likely to improve mass bias correction, as been shown in another isotope system and media.[30]
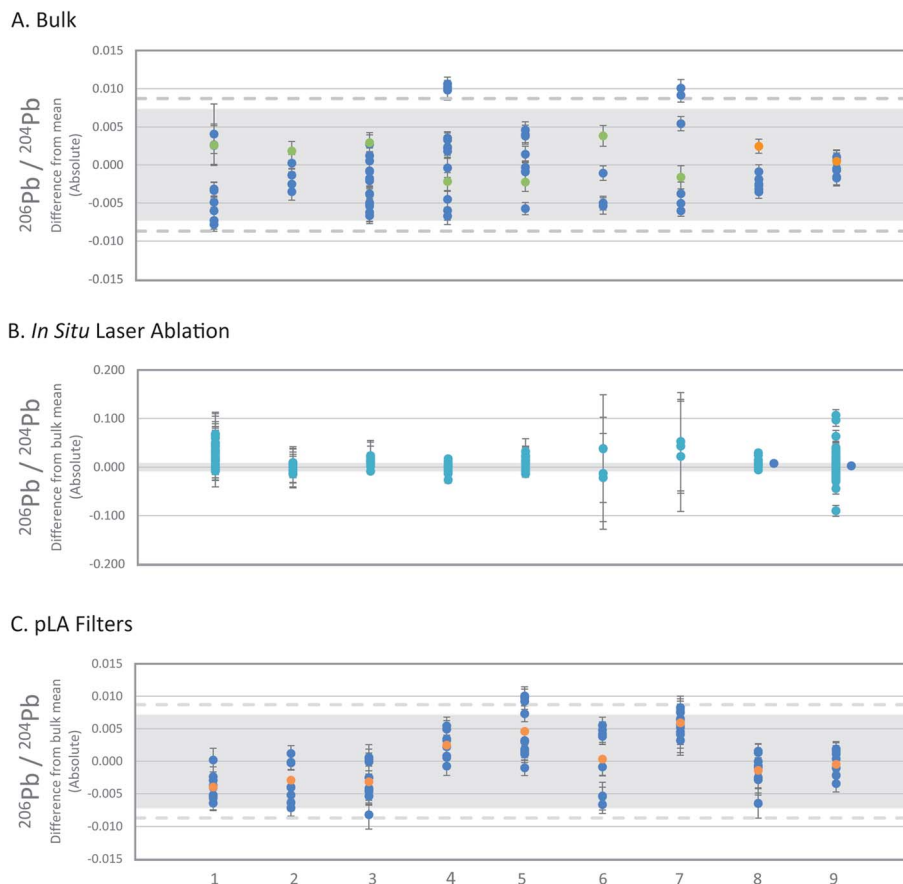
Results

Blanks

The filter blanks range from 60–480 pg, median 171 pg. The Pb blank for the columns was determined to be 20 pg, which is routinely achieved for the clean laboratory work (*i.e.*, sample digestion and ion-exchange chromatography).[24] Compared to the estimated 1 μg of Pb collected per filter, the total blank contribution is insignificant (<0.05%).

Bulk analyses

The long-term reproducibility of standard solution measurements of three laboratories (VU, Oxford, GU-Frankfurt am Main) that carried out bulk analyses of reference materials are comparable. The long-term precision of the Oxford laboratory based on 365 analyses over 1.5 years is 0.0041 $^{206}Pb/^{204}Pb$, 0.0031 for $^{207}Pb/^{204}Pb$, 0.0108 for $^{208}Pb/^{204}Pb$, 0.00015 for $^{207}Pb/^{206}Pb$ and 0.0005 for $^{208}Pb/^{206}Pb$ (2SD absolute). The combined propagated error for the three laboratories is 0.0071 $^{206}Pb/^{204}Pb$, 0.0060 for $^{207}Pb/^{204}Pb$, 0.0204 for $^{208}Pb/^{204}Pb$, 0.00024 for $^{207}Pb/^{206}Pb$ and 0.0006 for $^{208}Pb/^{206}Pb$ (2SD absolute). The bulk means were calculated by combining the bulk

Table 4 Average lead isotope ratios of reference materials using the pLA-filter-solution MC-ICPMS technique, VU Amsterdam. Averages and 2SD of 8-10 filters

		$^{206}Pb/^{204}Pb$	2SD	$^{207}Pb/^{204}Pb$	2SD	$^{208}Pb/^{204}Pb$	2SD	$^{207}Pb/^{206}Pb$	2SD	$^{208}Pb/^{206}Pb$	2SD
1	RMAg981-3	16.938	0.004	15.491	0.005	36.701	0.015	0.91459	0.00011	2.1668	0.0004
2	MBH 133X-AGA-3	17.409	0.006	15.547	0.009	37.279	0.028	0.89307	0.00023	2.1413	0.0009
3	RMAgD-1	18.688	0.005	15.658	0.006	38.788	0.020	0.83785	0.00009	2.0755	0.0005
4	RMAgN-2	18.510	0.004	15.642	0.005	38.650	0.017	0.84504	0.00008	2.0880	0.0004
5	RMAgS-1	18.051	0.008	15.585	0.010	38.106	0.030	0.86340	0.00014	2.1110	0.0007
6	RMAgC-2	18.531	0.010	15.640	0.012	38.480	0.038	0.84398	0.00020	2.0765	0.0010
7	RMAgP-2	20.075	0.003	15.823	0.003	40.982	0.011	0.78822	0.00006	2.0414	0.0003
8	RMAg3834	18.448	0.005	15.640	0.003	38.474	0.011	0.84777	0.00022	2.0855	0.0005
9	RMAg12467	18.532	0.004	15.662	0.004	38.647	0.015	0.84510	0.00011	2.0854	0.0004

152 | *J. Anal. At. Spectrom.*, 2022, **37**, 148–156

This journal is © The Royal Society of Chemistry 2022

Fig. 3 Comparison of $^{206}Pb/^{204}Pb$ of the three sampling methods. All Pb isotope ratios are shown in Fig. S1–S3.† The *x*-axis numbers refer to the reference materials as listed in Table 1. (A) Deviation of single bulk analyses of reference materials from inter-laboratory means. Error bars represent 2SE uncertainties of single bulk analyses. Propagated 2SD uncertainties of the inter-laboratory mean values are based on the long-term precision of standard solutions (grey; see text) and the maximum variation (2SD) of bulk analyses (dashed line). OX = blue, VU = green, GU F/M = orange. (B) Deviation of single *in situ* LA-MC-ICPMS analyses from inter-laboratory means. Error bars represent 2SE of single analyses. Propagated 2SD uncertainties of the inter-laboratory mean values are based on the long-term precision of standard solutions (grey; see text). nsLA = turquoise, fsLA = blue. (C) Deviation of pLA filter analyses compared to inter-laboratory means. Error bars on data symbols represent 2SE uncertainties of single analyses. Uncertainties of the inter-laboratory mean values are given as propagated 2SD based on the long-term precision of standard solutions (grey; see text), and maximum variation (2SD) of bulk analyses of the reference materials (dashed line). Filters = blue, filter mean = orange.

averages of each laboratory. The VU bulk analyses (Table 3) are within the combined propagated error relative to the inter-laboratory mean (Fig. 3a and S1†). By comparing the individual bulk analyses from the VU and Oxford laboratories, however, the variation is higher than can be explained by instrumental precision alone. The maximum variation seen in the bulk analyses is 0.0087 $^{206}Pb/^{204}Pb$, 0.0100 for $^{207}Pb/^{204}Pb$, 0.0276 for $^{208}Pb/^{204}Pb$, 0.00029 for $^{207}Pb/^{206}Pb$ and 0.0008 for $^{208}Pb/^{206}Pb$ (2SD absolute). These values more accurately represent the expected variance within and between laboratories.

In situ LA-MC-ICPMS

The *in situ* nsLA analyses consistently show a wider variation of lead isotope ratios than the bulk analyses, but the level of variation is specific to the individual reference materials (Fig. 3b and S2†). Of the 158 individual nsLA analyses of reference

materials spread across three laboratories, 3 analyses failed the Grubb's outlier test and are excluded from further discussion (grey highlight in Tables S5 and S6†).

The variation from the mean (2SD absolute) of all *in situ* nsLA analyses of each reference material fall between 0.016–0.062 for $^{206}Pb/^{204}Pb$, 0.015–0.051 for $^{207}Pb/^{204}Pb$, 0.043–0.148 for $^{208}Pb/^{204}Pb$, 0.00008–0.00109 for $^{208}Pb/^{206}Pb$ and 0.0005–0.00037 for $^{208}Pb/^{206}Pb$. The maximum variation of the *in situ* nsLA analyses is five-times higher than the bulk analyses for ^{204}Pb-normalised ratios. The lower precision is recorded in the variability of repeat measurements within individual laboratories rather than the variability between laboratories. The standard deviations of all *in situ* nsLA analyses for each reference material are smaller or the same as the maximum standard deviation of the analyses within any single laboratory.

For all reference materials, the inter-laboratory *in situ* nsLA averages (±2SD) are accurate within the maximum uncertainty (2SD) of the bulk inter-laboratory average, taken to be the 'true'

value. Intra-laboratory *in situ* nsLA averages (±2SD) are accurate in almost every case. The $^{206}Pb/^{204}Pb$ ratios of RMAgP-1 (Southampton) and two of RMAgD-1 (Southampton and University of Edinburgh) and the $^{207}Pb/^{206}Pb$ ratios of RMAgC-1 and RMAgP-1 (Southampton) fall outside of range of the 'true' value (60%, 42%, 14%, 39% and −33%, respectively, greater or less than the maximum 2SD of the bulk analyses).

The nsLA measurements of reference materials MBH-AGA3, RMAgN-2 and RMAgS-1, which were analysed in two or three laboratories, are particularly precise and accurate. The Southampton analyses of RMAgP-1 and RMAgC-1 indicated a high degree of isotopic heterogeneity during ablation, which was not seen in any other reference material. These two reference materials were made by doping the silver with archaeological lead, unlike other reference materials, so the heterogeneity observed likely stems from how these two reference materials were made. They were subsequently homogenised by re-melting but were not analysed further by *in situ* LA.

The fsLA analyses of archaeological reference materials RMAg3834 and RMAg12467 are accurate, both falling within the combined propagated uncertainty of the 'true' value inter-laboratory bulk average.

Indirect pLA-solution method

The average isotopic compositions obtained from the results of 8–10 laser-ablated sample (replicates) for each silver set, are presented in Table 3 and the individual analyses of each set of ablations in Table S1.† Analysis of the data obtained *via* pLA for each individual silver standard established that RMAg981-3, RMAgD-1, RMAgS-1 and RMAg12467 have a single filter analysis that fails the Grubb's outlier test (grey highlight in Table S1†).

After rejecting these measurements (4 of 86), the averages of individual silver set (2SD) are within error (2SD) of the propagated inter-laboratory long-term precision, with exception of RMAgP-2, but the measurement uncertainties (2SD) nevertheless overlap with the maximum uncertainty (2SD) of inter-laboratory bulk analysis (Fig. 3c and S3†). The uncertainties of the individual silver sets (2SD) is almost comparable in every case to the uncertainties (2SD) of the inter-laboratory bulk analyses. RMAgC-2 has higher uncertainties than the maximum uncertainties of the bulk analyses (10–39% greater than 2SD for four of the five isotope ratios).

Microscopic examination of the ablation craters and the ablated material indicates that the laser caused melting to occur (Fig. 2). Spherical droplets of up to ∼2 μm of metallic silver were widespread (<5%) on the filters. The consistent isotopic data, however, demonstrate that the melting effects were not strong enough to impart quantifiable isotopic fractionation. While melting of the matrix and the compositional heterogeneity of the ablated standards may be sources of error for *in situ* nsLA-MC-ICPMS analysis, these issues appear to be circumvented through the digestion of the pLA-filter.

The individual filter analyses of each reference material are strongly correlated (Fig. 4 and S4†) and nearly all variance is consistent with mass-dependent fractionation, which is typical
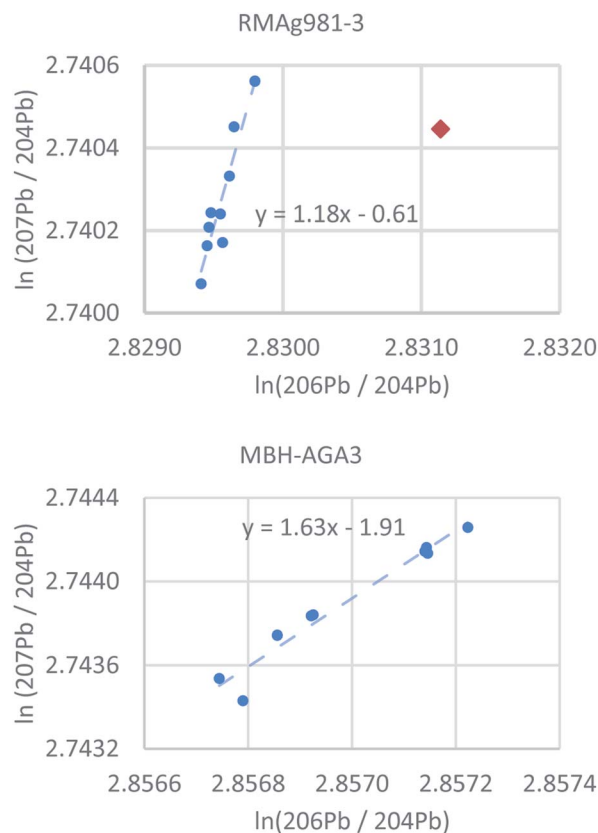

Fig. 4 Logarithmic representations of lead isotope ratios of individual pLA filters using two reference materials as examples (all reference materials are shown in Fig. S4†). Nearly all analyses fall on arrays consistent with mass-dependent fractionation. Red diamond = statistical outlier.

for datasets corrected using the standard sample bracketing method. Four filters (4 of 86) do not fall on mass-dependent fractionation lines, three of which are statistical outliers mentioned above. These are single filters from RMAg981-3 (true outlier), RMAgN-2 (true outlier), RMAgD-1 (true outlier) and RMAg3834. The nonconformity of these four filters is probably caused by external contamination or a memory effect. The ratios of the fourth true statistical outlier, a single filter from RMAg12467, fall on projected mass-dependent fractionation lines, but the source of error is unknown.

The study found no correlation between the qualities of the Pb isotope data, assessed as the correct lead isotope ratio, and the different column batches, number of ablations per filter (2–10) and the different silver matrices. In particular, the potential influence of different matrix compositions, reflected by the amount of silver present in the sample solution during MC-ICPMS analyses, were evaluated. Due to incomplete chromatography separation during chemistry purification, variable amounts of the silver matrix may remain in the measurement solution. Potential offset of lead isotope ratios from the correct values was evaluated by doping a NIST981 solution with Ag (Table S9†). The test showed the appearance of an isotopic offset from the correct lead isotope ratios when the Ag/Pb ratio was above 30 : 1. However, the silver standards do not record

154 | *J. Anal. At. Spectrom.*, 2022, **37**, 148–156

This journal is © The Royal Society of Chemistry 2022

any correlation between Pb isotope and Ag/Pb ratios, indicating no simple correlation with the solution matrix. These results were expected as the sample solutions typically had Ag/Pb ratios significantly less than 30 (Table S1†). Only three sample aliquots recorded Ag/Pb values ≥ 30 (one each of RMAg981-3, RMAgD-1 and RMAgC-1), but record no systematic isotopic offset. The limited data in this study with high Ag/Pb ratio suggest that the silver present in the matrix did not affect the data quality. It is recommended, however, that the Ag/Pb ratio should be quantitatively assessed in future studies and a larger dataset obtained.

Discussion

In nearly every case, repeated pLA-filter sampling produced precisions comparable to the precision of bulk analyses processed in different laboratories and typically have a precision that is more than five-times better than *in situ* nsLA-MC-ICPMS. Assuming the inter-laboratory bulk means represent the 'true' values, the filter means (±2SD) are accurate within the maximum variation (±2SD) observed in the bulk analyses. Laser-induced fractionation or sample heterogeneity appears to have played no detectable role in the precision and accuracy of the filter measurements. Small offsets in reference to the VU bulk analyses can be seen in the filter sets, but this variation is certainly not blank controlled because the highest and lowest Pb-isotope ratios are offset in different directions.

When working with such small samples (~1 μg Pb), the principal hazard is contamination. A potential source of contamination are traces of ablated material adhering to the equipment (tubing, sample/filter holder, elements of the laser ablation module), emphasizing the need for adequate cleaning. One of the statistical outliers (RMAg981-3) was the first analysis after the ablation of (highly radiogenic) RMAgP-2, and could reflect traces of the previous sample (memory effect). The other three statistical outliers are the last filter of the series and are inconsistent with a direct memory effect. The origin of the outliers is therefore unclear. The low frequency of significant outliers (4 of 86 filters, ~5%) is acceptable, but it may be possible to lower this through additional cleaning measures. Outliers occur in ~2% of the *in situ* nsLA-MC-ICPMS analyses, but the added precision and accuracy made possible by solution-based sample preparation makes the analytical capabilities of the pLA-filter-digestion approach superior to *in situ* nsLA analysis.

For the practical application of pLA sampling, it is recommended that two or three filters be collected per object to ensure the reliability of the data. Assuming that the data presented here is representative, there is a 5% chance that a single filter would be a statistical outlier. Of the 82 filters (95%) that are not outliers, 19 filters (24%) have at least one isotope ratio straying more than ±2SD from the inter-laboratory bulk mean (2SD = maximum uncertainty seen in the bulk analyses), one (1%) with all isotope ratios falling between ±2SD and ±3SD, and two (2%) with a single isotope ratio straying more than ±3SD. A set of three filters would allow potential outliers to be identified, and two or three filters with lead isotope ratios within the expected precision range would signal that the results are reliable. A balance must be struck between the number of filter repetitions and total ablations, the reliability of the analytical results and the impact to an archaeological artefact.

Conclusions

The aim of the study was to test the analytical potential of pLA sampling on archaeological silver for lead isotope analysis. The results show that virtually non-invasive micro-sampling by laser is a way to obtain highly precise and accurate lead isotope data while circumventing a number of analytical, logistical, curatorial and form-dependent factors that limit the efficacy of *in situ* LA analysis for archaeological and museum objects. Sampling *via* pLA for lead isotope analysis requires a reliable estimate of the lead concentration in the silver so that the number of ablations can be adjusted to ensure a collection of ≥1 μg Pb. The normal range of lead in archaeological silver is between 0.5–1.0 wt% Pb, which equates to 4 to 8 ablations per filter. Sampling silver with <0.35 wt% Pb would require more than 10 ablations per filter and were not tested in this study, though there is nothing to suggest that this would be unsuccessful. Given these prerequisites, pLA sampling for lead isotope analysis has the potential for extensive applications in the field of archaeological science, opening up access to a large pool of unstudied artefacts from museum collections worldwide.

Conflicts of interest

There are no conflicts to declare.

Acknowledgements

References

1 F. Albarede, J. Blichert-Toft, L. Gentelli, J. Milot, M. Vaxevanopoulos, S. Klein, K. Westner, T. Birch, G. Davis and F. de Callataÿ, A miner's perspective on Pb isotope provenances in the Western and Central Mediterranean, *J. Archaeol. Sci.*, 2020, **121**, DOI: 10.1016/j.jas.2020.105194.

2 D. J. Killick, J. A. Stephens and T. R. Fenn, Geological constraints on the use of lead isotopes for provenance in archaeometallurgy, *Archaeometry*, 2020, **62**(S1), 86–105.

3 Z. A. Stos-Gale and N. H. Gale, Metal provenancing using isotopes and the Oxford archaeological lead isotope database (OXALID), *Archaeol. Anthropol. Sci.*, 2009, **1**, 195–213.

This journal is © The Royal Society of Chemistry 2022

J. Anal. At. Spectrom., 2022, **37**, 148–156 | **155**

4 F. Albarède, J. Blichert-Toft, M. Rivoal and P. Telouk, A glimpse into the Roman finances of the Second Punic War through silver isotopes, *Geochem Perspect Lett.*, 2016, **2**, 127–137.

5 J. Baker, S. Stos and T. Waight, Lead isotope analysis of archaeological metals by multiple-collector inductively coupled plasma mass spectrometry, *Archaeometry*, 2006, **48**(1), 45–56.

6 M. Burger, R. Glaus, V. Hubert, S. van Willigen, M. Wörle-Soares, F. Convertini, P. Lefranc, E. Nielsen and D. Günther, Novel sampling techniques for trace element quantification in ancient copper artifacts using laser ablation inductively coupled plasma mass spectrometry, *J. Archaeol. Sci.*, 2017, **82**, 62–71.

7 A. A. Gordus, Neutron activation analysis of coins and coin streaks, in *Methods of Chemical and Metallurgical Investigation of Ancient Coinage*, ed. E. T. Hall and D. M. Metcalf, Royal Numismatics Society, 1972, pp. 127–148.

8 M. F. Guerra, C.-O. Sarthre, A. Gondonneau and J.-N. Barrandon, Precious Metals and Provenance Enquiries using LA-ICP-MS, *J. Archaeol. Sci.*, 1999, **26**(8), 1101–1110.

9 R. W. Law and J. H. Burton, Nondestructive Pb isotope sampling and analysis of archaeological silver using EDTA and ICP-MS, *Am. Lab.*, 2008, **40**(17), 14–15.

10 F. Schweizer, Analysis of ancient coins using a point source linear X-ray spectrometer: A critical review, in *Methods of Chemical and Metallurgical Investigation of Ancient Coinage*, ed. E. T. Hall and D. M. Metcalf, Royal Numismatics Society, 1972, pp. 153–169.

11 R. Lehmann, Archäometallurgie von mittelalterlichen deutschen Silberbarren und Münzen, Doctoral thesis, Leibniz Universität Hannover, 2011.

12 E. Pernicka, F. Begemann, S. Schmitt-Strecker and A. P. Grimanis, On the composition and provenance of metal artefacts from Poliochni on Lemnos, *Oxford J. Archaeol.*, 1990, **9**(3), 263–298.

13 C. D. Standish, S. W. Merkel, Y.-T. Hsieh and J. Kershaw, Simultaneous lead isotope ratio and gold-lead-bismuth concentration analysis of silver by laser ablation MC-ICP-MS, *J. Archaeol. Sci.*, 2021, **125**, DOI: 10.1016/j.jas.2020.105299.

14 R. Glaus, L. Dorta, Z. Zhang, Q. Ma, H. Berke and D. Günter, Isotope ratio determination of objects in the field by portable laser ablation sampling and subsequent multicollector ICPMS, *J. Anal. At. Spectrom.*, 2013, **28**, 801–809.

15 M. Ponting, J. A. Evans and V. Pashley, Fingerprinting of Roman mints using laser-ablation MC-ICP-MS lead isotope analysis, *Archaeometry*, 2003, **45**(4), 591–597.

16 J. Kershaw, S. W. Merkel, J. Oravisjarvi, E. Kooijman and M. Schmidt, The scale of dirham imports to the Swedish Baltic in the ninth century: new evidence from archaeometric analysis of early Viking-age silver, *Fornvännen*, 2021, **116**, 185–204.

17 J. Kershaw and S. W. Merkel, *The Galloway Hoard: Elemental and Isotopic Analyses*. Unpublished report, National Museum of Scotland, 2020.

18 I. Horn and F. von Blanckenburg, Investigation on elemental and isotopic fractionation during 196 nm femtosecond laser ablation multiple collector inductively coupled plasma mass spectrometry, *Spectrochim. Acta, Part B*, 2007, **62**(4), 410–422.

19 S. E. Jackson and D. Günther, The nature and source of laser induced isotopic fractionation in laser ablation-multicollector-inductively coupled plasma-mass spectrometry, *J. Anal. At. Spectrom.*, 2003, **18**, 205–212.

20 N. J. Saetveit, S. J. Bajic, D. P. Baldwin and R. S. Houk, Influence of particle size on fractionation with nanosecond and femtosecond laser ablation in brass by online differential mobility analysis and inductively coupled plasma mass spectrometry, *J. Anal. At. Spectrom.*, 2008, **23**, 54–61.

21 A. C. S. Knaf, J. M. Koornneef and G. R. Davies, "Non-invasive" portable laser ablation sampling of art and archaeological materials with subsequent Sr-Nd isotope analysis by TIMS using 10^{13} Ω amplifiers, *J. Anal. At. Spectrom.*, 2017, **32**, 2210–2216.

22 R. Glaus, J. Koch and D. Günther, Portable laser ablation sampling device for elemental fingerprinting of objects outside the laboratory with laser ablation inductively coupled plasma mass spectrometry, *Anal. Chem.*, 2012, **84**, 5358–5364.

23 S. W. Merkel, Evidence for the widespread use of dry silver ore in the early Islamic period and its implications for the history of silver metallurgy, *J. Archaeol. Sci.*, 2021, **135**, DOI: 10.1016/j.jas.2021.105478.

24 J. M Koornneef, I. Nikogosian, M. J. van Bergen, P. Z. Vroon and G. R. Davies, Ancient recycled lower crust in the mantle source of recent Italian magmatism, *Nat. Com.*, 2019, **10**(1), 3237.

25 M. U. Gress, J. M. Koornneef, E. Thomassot, I. L. Chinn, K. van Zuilen and G. R. Davies, Sm-Nd isochron ages coupled with C-N isotope data of eclogitic diamonds from Jwaneng, Botswana, *Geochim. Cosmochim. Acta*, 2021, **293**, 1–17.

26 P. d'Imporzano, K. Keune, J. M. Koornneef, E. Hermens, P. Noble, K. van Zuilen and G. R. Davies, Micro-invasive method for studying lead isotopes in paintings, *Archaeometry*, 2020, **62**(4), 796–809.

27 M. F. Thirlwall, Multicollector ICP-MS analysis of Pb isotopes using a 207Pb-204Pb double spike demonstrates up to 400 ppm/amu systematic errors in Tl-normalization, *Chem. Geol.*, 2002, **184**, 255–279.

28 S. W. Merkel, *Silver and the Silver Economy at Hedeby*, Marie Leidorf, 2016.

29 S. W. Merkel, Provenancing Viking Silver: Methodological and Theoretical Considerations and a Case Study, in *Silver, Butter, Cloth: Monetary and Social Currencies in the Viking Age*, ed. J. Kershaw and G. Williams, Oxford University Press, 2019, pp. 206–226.

30 V. Devulder, A. Gerdes, F. Vanhaecke and P. Degryse, Validation of the determination of the B isotopic composition in Roman glasses with laser ablation multi-collector inductively coupled plasma-mass spectrometry, *Spectrochim. Acta, Part B*, 2015, **105**, 116–120.

156 | *J. Anal. At. Spectrom.*, 2022, **37**, 148–156

This journal is © The Royal Society of Chemistry 2022